Theoretical studies on α-decay half-lives of $N = 125$, 126, and 127 isotones

Zhen Wang,[1] Zhongzhou Ren,[1,2,*] and Dong Bai[1]

[1]*School of Physics Science and Engineering, Tongji University, Shanghai 200092, China*

[2]*Key Laboratory of Advanced Micro-Structure Materials, Ministry of Education, Shanghai 200092, China*

(Received 14 January 2020; revised manuscript received 30 March 2020; accepted 27 April 2020; published 15 May 2020)

The α decays of exotic $N = 125$, 126, and 127 isotones, including two new isotopes ^{219}Np [Phys. Lett. B **777**, 212 (2018)] and ^{220}Np [Phys. Rev. Lett. **122**, 192503 (2019)], are studied by using the improved Buck-Merchant-Perez cluster model with the charge-dependent α-preformation factors. The experimental half-lives of α decays varying from 2.50×10^{-5} to 6.00×10^{26} s are reproduced within a factor of $\approx$2. Noticeably, the theoretical α-decay half-lives of the new isotopes ^{219,220}Np are also in good agreement with the experimental data. Furthermore, the α-decay half-lives of some undiscovered $N = 125$, 126 and 127 isotones are predicted, which could be useful for future experimental studies on the robustness of the magic number $N = 126$.

DOI: 10.1103/PhysRevC.101.054310

I. INTRODUCTION

α decay is an important decay mode for unstable nuclei [1–4]. Theoretically, α decay is often described in two steps. First, an α cluster is preformed and trapped temporarily inside the parent nucleus, with the preformation probability given by the so-called α-preformation factor P_α. Then, the α cluster escapes from the parent nucleus through the quantum tunneling effect, which completes the α-decay process. Various phenomenological and microscopic models have been proposed in the literature to study the α decay and the relevant α-clustering effect across the nuclide chart, such as the Buck-Merchant-Perez (BMP) cluster model [5–7], the cluster-configuration shell model [8,9], the density-dependent cluster model [10] (see also Ref. [11]), the generalized density-dependent cluster model [12], the quartetting wave-function approach [13], the unified model for α decay and α capture [14], the quartet model [15], the quartet condensation model [16], etc. α decay provides rich information on nuclear structure and is essential for identifying the new superheavy elements. Especially, it is shown in, e.g., Refs. [17–30] that the variation of α-decay data along the isotopic and isotonic chains provides a sensitive probe of magic numbers and helps deepen our understanding of the evolution of shell structures.

The $N = 126$ neutron major shell plays a crucial role in understanding the physical properties of heavy and superheavy elements. Its robustness on the proton-rich side is an important open question in modern nuclear physics. Recently, two new short-lived isotopes ^{219}Np ($Q_\alpha = 9.207$ MeV, $T_{1/2}^{\rm Expt} = 1.50 \times 10^{-4}$ s) and ^{220}Np ($Q_\alpha = 10.226$ MeV, $T_{1/2}^{\rm Expt} = 2.50 \times 10^{-5}$ s) have been reported in Refs. [23,24]. Combining these new experimental data with the previous data, a systematical study is carried out of the variation of the α-decay data along the Np isotopic chain, which provides important evidence on the robustness of the magic number $N = 126$ in the Np isotopes [24].

In this work, we present a systematic study of α decays of $N = 125$, 126, and 127 isotones by using the improved BMP cluster model with the charge-dependent α-preformation factors. In the original BMP cluster model, it is the constant α-preformation factors that are adopted in the theoretical calculations, with $P_\alpha^{\rm ee} = 1$, $P_\alpha^{\rm oe} = 0.6$, and $P_\alpha^{\rm oo} = 0.35$ for the even-even, odd-A, and odd-odd nuclei, respectively [6]. The charge-dependent α-preformation factors used in this work are based on a two-level model [31–37] and take into consideration the evolution of shell structures and the Pauli-blocking effect. The remaining parts of this paper are organized as follows: In Sec. II, we present the theoretical framework of the improved BMP cluster model with the charge-dependent α-preformation factors. In Sec. III, the numerical results for the α-decay half-lives of $N = 125$, 126, and 127 isotones, including the recently discovered ^{219,220}Np, are presented and discussed. We also make quantitative predictions on the α-decay half-lives for some undiscovered $N = 125$, 126, 127 isotones, which could be useful references for future experiments to probe the robustness of the magic number $N = 126$. Finally, a summary is given in Sec. IV.

II. THEORETICAL FRAMEWORK

In this section, we introduce the theoretical formalism of the improved BMP cluster model. Following Refs. [5–7], it is assumed that the α cluster is preformed first in the surface region of the parent nucleus, with the preformation probability given by the α-preformation factor P_α. The α cluster is trapped temporarily inside the Coulomb barrier and orbits around the daughter nucleus.

Due to the Pauli-blocking effect in quantum mechanics, the α-cluster orbits cannot enter the central region of the daughter

*zren@tongji.edu.cn

nucleus, which has already been occupied by the nucleons in the daughter nucleus. We adopt the Wildermuth condition [38] to implement the Pauli blocking approximately, which selects the physically allowed orbits with a global quantum number $G = 2n + L$. Here, n is the node number of the radial wave function of the α cluster, and L is the orbital angular momentum. Generally, the value of G varies from 18 to 24 for heavy and superheavy nuclei, and is changed by two when crossing the magic number [5–7].

The effective potential $V(r)$ between the α cluster and the daughter nucleus is given by

$$V(r) = V_N(r) + V_C(r) + V_L(r), \tag{1}$$

with $V_N(r)$ being the nuclear potential, $V_C(r)$ being the Coulomb potential, and $V_L(r)$ being the centrifugal potential. The nuclear potential is chosen to be the cosh potential [6,7],

$$V_N(r) = -V_0 \frac{1 + \cosh(R/a)}{\cosh(r/a) + \cosh(R/a)}. \tag{2}$$

In Eq. (2), $V_0 = 162.3$ MeV describes the depth of the potential, $a = 0.40$ fm is the diffuseness parameter, and R denotes the radius of the daughter nucleus to be determined later on. The Coulomb potential between the α cluster and the daughter nucleus is given by

$$V_C(r) = \begin{cases} \frac{Z_1 Z_2 e^2}{r} & (r \geqslant R) \\ \frac{Z_1 Z_2 e^2}{2R}\left[3 - \left(\frac{r}{R}\right)^2\right] & (r \leqslant R), \end{cases} \tag{3}$$

where Z_1 and Z_2 are the charges of the α particle and the daughter nucleus, respectively.

The centrifugal potential is given by

$$V_L(r) = \frac{\hbar^2}{2\mu r^2}\left(L + \frac{1}{2}\right)^2 \tag{4}$$

in the Langer approximation [39]. Here, $\mu = \frac{m_d m_\alpha}{m_d + m_\alpha}$ is the reduced mass of the two-body system of the α cluster and the daughter nucleus, with m_d and m_α being the mass of the daughter nucleus and the α particle, respectively. The conservation laws of angular momentum and parity demand that

$$|I_f - I_i| \leqslant L \leqslant I_f + I_i, \quad \frac{\pi_f}{\pi_i} = (-1)^L, \tag{5}$$

where I_i, I_f, π_i, π_f are the spins and parities of the initial and final states, respectively.

The dynamics of the two-body system of the α cluster and the daughter nucleus could be obtained in a semiclassical approach. The motion of an α cluster inside the parent nucleus is determined by the Bohr-Sommerfeld quantization condition

$$\int_{r_1}^{r_2} dr \sqrt{\frac{2\mu}{\hbar^2}[Q_\alpha - V(r)]} = (G - L + 1)\frac{\pi}{2}, \tag{6}$$

where r_1, r_2, and r_3 are the first, second, and third classical turning points with increasing distances from the center of the daughter nucleus.

As mentioned before, G is the global quantum number that selects the physically allowed orbits and ranges from 18 to 24 for various nuclei in the literature. In this work, we take

$$G = \begin{cases} 24 & \text{for } N > 126 \\ 22 & \text{for } 82 < N \leqslant 126 \\ 20 & \text{for } N \leqslant 82, \end{cases} \tag{7}$$

for parity-preserving α decays. As noted in, e.g., Ref. [37], the global quantum number G should take odd values for parity-changing α decays. In these cases, we take $G = 23$ for $N > 126$ and $G = 21$ for $N \leqslant 126$. Given the Q_α values, the classical turning points and the radius R could be found from Eq. (6). The α-decay width Γ_α is given by [5–7]

$$\Gamma_\alpha = P_\alpha F \frac{\hbar^2}{4\mu} \exp\left[-2\int_{r_2}^{r_3} dr k(r)\right], \tag{8}$$

with F being the normalization factor [40]

$$F = \left[\int_{r_1}^{r_2} dr \frac{1}{2k(r)}\right]^{-1}, \tag{9}$$

and $k(r)$ being the wave number

$$k(r) = \sqrt{\frac{2\mu}{\hbar^2}|Q_\alpha - V(r)|}. \tag{10}$$

The α decay half-life is then related to the decay width by

$$T_{1/2} = \frac{\hbar \ln 2}{\Gamma_\alpha}. \tag{11}$$

Compared with the quantum-tunneling stage, the preformation of the α cluster is less known theoretically. Often, the α-preformation factor is adopted to measure the probability of the α-cluster preformation. In the original BMP cluster model, the constant α-preformation factors are used in the theoretical calculations, with $P_\alpha^{\mathrm{ee}} = 1$, $P_\alpha^{\mathrm{oe}} = 0.6$, and $P_\alpha^{\mathrm{oo}} = 0.35$ for the even-even, odd-A, and odd-odd nuclei, respectively. This choice could be regarded as the zeroth-order approximation of the realistic α-preformation factors. In this work, we make improvements by adopting the charge-dependent α-preformation factors inspired by previous studies based a microscopic two-level model, which considers the pairing forces between nucleons and the impact of the shell structures and the Pauli blocking. Explicitly, along an isotonic chain we have [31–37]

$$P_\alpha = C Z_v (1 - Z_v/\Omega). \tag{12}$$

In Eq. (12), C is a constant to be determined for each isotonic chain, Z_v is the valence proton number, and $(1 - Z_v/\Omega)$ represents the effect of the Pauli blocking, with Ω being the maximum proton number in a major shell. As Ω is often much larger than Z_v [31–37], for isotones around the $N = 126$ shell closure Eq. (12) can be further simplified as

$$P_\alpha \approx C(Z - 82). \tag{13}$$

The α-preformation factor could also be estimated by using other models. For example, Refs. [13,15,29] estimate the α-preformation factor in terms of the norm of the α-cluster relative wave function outside the so-called Mott radius, based on the simplified picture that the α cluster retains its identity only outside the Mott radius and gets dissolved and

TABLE I. Calculations of the α-decay half-lives of the $N = 125$, 126, and 127 isotones with $83 \leqslant Z \leqslant 93$, from ground state to ground state. "#" in the table means that the spin and parity of this nuclide are obtained from trends in neighboring nuclides with the same Z and N particles, and "()" means uncertain spin and/or parity. $T_{1/2}^{\rm Expt}$ denotes the experimental half-lives, $T_{1/2}^{\rm C\text{-}P}$ and $T_{1/2}^{\rm Z\text{-}P}$ denote the theoretical half-lives calculated by using the original BMP cluster model with the constant α-preformation factors $P_\alpha^{\rm C}$ and the improved BMP cluster model with the charge-dependent α-preformation factors $P_\alpha^{\rm Z}$, respectively.

α decay	I_i^π	I_f^π	L	Q_α (MeV)	$P_\alpha^{\rm Z}$	$T_{1/2}^{\rm Expt}$ (s)	$T_{1/2}^{\rm C\text{-}P}$ (s)	$T_{1/2}^{\rm Z\text{-}P}$ (s)
$N = 125$ (odd-A), $P_\alpha^{\rm C} = 0.6$, $P_\alpha^{\rm Z} = 0.0239(Z-82)$								
^{217}U $\rightarrow$ ^{213}Th $+\alpha$[a]	$1/2^-$#	$5/2^-$#	2	8.428	0.2390	1.60×10^{-2}	9.43×10^{-3}	2.37×10^{-2}
^{215}Th $\rightarrow$ ^{211}Ra $+\alpha$	$(1/2^-)$	$5/2(^-)$	2	7.665	0.1912	1.20×10^{0}	3.83×10^{-1}	1.21×10^{0}
^{213}Ra $\rightarrow$ ^{209}Rn $+\alpha$	$1/2^-$	$5/2^-$	2	6.862	0.1434	2.05×10^{2}	4.28×10^{1}	1.79×10^{2}
^{211}Rn $\rightarrow$ ^{207}Po $+\alpha$	$1/2^-$	$5/2^-$	2	5.965	0.0956	1.92×10^{5}	3.52×10^{4}	2.21×10^{5}
^{209}Po $\rightarrow$ ^{205}Pb $+\alpha$	$1/2^-$	$5/2^-$	2	4.979	0.0478	3.91×10^{9}	6.30×10^{8}	7.91×10^{9}
$N = 125$ (odd-odd), $P_\alpha^{\rm C} = 0.35$, $P_\alpha^{\rm Z} = 0.0144(Z-82)$								
^{216}Pa $\rightarrow$ ^{212}Ac $+\alpha$	5^+#	6^+#	2	8.097	0.1296	1.05×10^{-1}	6.69×10^{-2}	1.81×10^{-1}
^{214}Ac $\rightarrow$ ^{210}Fr $+\alpha$	5^+#	6^+	2	7.352	0.1008	9.21×10^{0}	3.04×10^{0}	1.05×10^{1}
^{212}Fr $\rightarrow$ ^{208}At $+\alpha$	5^+	6^+	2	6.529	0.0720	2.79×10^{3}	5.72×10^{2}	2.78×10^{3}
^{210}At $\rightarrow$ ^{206}Bi $+\alpha$	$(5)^+$	$6(^+)$	2	5.631	0.0432	1.67×10^{7}	8.48×10^{5}	6.87×10^{6}
$N = 126$ (even-even), $P_\alpha^{\rm C} = 1$, $P_\alpha^{\rm Z} = 0.0306(Z-82)$								
^{218}U $\rightarrow$ ^{214}Th $+\alpha$	0^+	0^+	0	8.775	0.3060	5.50×10^{-4}	3.37×10^{-4}	1.10×10^{-3}
^{216}Th $\rightarrow$ ^{212}Ra $+\alpha$	0^+	0^+	0	8.072	0.2448	2.60×10^{-2}	6.55×10^{-3}	2.67×10^{-2}
^{214}Ra $\rightarrow$ ^{210}Rn $+\alpha$	0^+	0^+	0	7.273	0.1836	2.44×10^{0}	4.35×10^{-1}	2.37×10^{0}
^{212}Rn $\rightarrow$ ^{208}Po $+\alpha$	0^+	0^+	0	6.385	0.1224	1.43×10^{3}	1.56×10^{2}	1.27×10^{3}
^{210}Po $\rightarrow$ ^{206}Pb $+\alpha$	0^+	0^+	0	5.408	0.0612	1.20×10^{7}	7.30×10^{5}	1.19×10^{7}
$N = 126$ (odd-A), $P_\alpha^{\rm C} = 0.6$, $P_\alpha^{\rm Z} = 0.0252(Z-82)$								
^{219}Np $\rightarrow$ ^{215}Pa $+\alpha$[b]	$9/2^-$#	$9/2^-$#	0	9.207	0.2772	1.50×10^{-4}	9.13×10^{-5}	1.98×10^{-4}
^{217}Pa $\rightarrow$ ^{213}Ac $+\alpha$	$9/2^-$#	$9/2^-$#	0	8.489	0.2268	3.48×10^{-3}	1.53×10^{-3}	4.04×10^{-3}
^{215}Ac $\rightarrow$ ^{211}Fr $+\alpha$	$9/2^-$	$9/2^-$	0	7.746	0.1764	1.70×10^{-1}	4.69×10^{-2}	1.60×10^{-1}
^{213}Fr $\rightarrow$ ^{209}At $+\alpha$	$9/2^-$	$9/2^-$	0	6.905	0.1260	3.43×10^{1}	6.03×10^{0}	2.87×10^{1}
^{211}At $\rightarrow$ ^{207}Bi $+\alpha$	$9/2^-$	$9/2^-$	0	5.982	0.0756	6.21×10^{4}	5.35×10^{3}	4.25×10^{4}
^{209}Bi $\rightarrow$ ^{205}Tl $+\alpha$	$9/2^-$	$1/2^+$	5	3.137	0.0252	6.00×10^{26}	4.14×10^{25}	9.86×10^{26}
$N = 127$ (odd-A), $P_\alpha^{\rm C} = 0.6$, $P_\alpha^{\rm Z} = 0.0055(Z-82)$								
^{219}U $\rightarrow$ ^{215}Th $+\alpha$[a]	$9/2^+$#	$(1/2^-)$	5	9.940	0.0550	4.20×10^{-5}	4.27×10^{-6}	4.66×10^{-5}
^{217}Th $\rightarrow$ ^{213}Ra $+\alpha$	$9/2^+$#	$1/2^-$	5	9.435	0.0440	2.47×10^{-4}	1.43×10^{-5}	1.95×10^{-4}
^{215}Ra $\rightarrow$ ^{211}Rn $+\alpha$	$9/2^+$#	$1/2^-$	5	8.864	0.0330	1.67×10^{-3}	7.86×10^{-5}	1.43×10^{-3}
^{213}Rn $\rightarrow$ ^{209}Po $+\alpha$	$9/2^+$#	$1/2^-$	5	8.245	0.0220	1.95×10^{-2}	7.13×10^{-4}	1.95×10^{-2}
^{211}Po $\rightarrow$ ^{207}Pb $+\alpha$	$9/2^+$	$1/2^-$	5	7.595	0.0110	5.16×10^{-1}	1.08×10^{-2}	5.91×10^{-1}
$N = 127$ (odd-odd), $P_\alpha^{\rm C} = 0.35$, $P_\alpha^{\rm Z} = 0.0035(Z-82)$								
^{220}Np $\rightarrow$ ^{216}Pa $+\alpha$[c]	1^-#	5^+#	5	10.226	0.0385	2.50×10^{-5}	3.52×10^{-6}	3.20×10^{-5}
^{218}Pa $\rightarrow$ ^{214}Ac $+\alpha$	1^-#	5^+#	5	9.815	0.0315	1.13×10^{-4}	6.78×10^{-6}	7.53×10^{-5}
^{216}Ac $\rightarrow$ ^{212}Fr $+\alpha$	(1^-)	5^+	5	9.235	0.0245	4.40×10^{-4}	3.47×10^{-5}	4.96×10^{-4}
^{214}Fr $\rightarrow$ ^{210}At $+\alpha$	(1^-)	$(5)^+$	5	8.589	0.0175	5.18×10^{-3}	3.17×10^{-4}	6.35×10^{-3}
^{212}At $\rightarrow$ ^{208}Bi $+\alpha$	(1^-)	5^+	5	7.817	0.0105	3.14×10^{-1}	9.26×10^{-3}	3.09×10^{-1}

[a]The experimental data are taken from Ref. [42].
[b]The experimental data are taken from Ref. [23].
[c]The experimental data are taken from Ref. [24].

merges with shell-model structures inside the Mott radius. In Ref. [41], the α-preformation factor is estimated by using the cluster-formation model as the ratio between the formation energy of the α cluster and the total energy of the four-nucleon system. Reference [30] proposes some analytic formulas for the α-preformation factor, which takes into consideration the impacts of the shell structures and can be a helpful reference for microscopic studies. Equations (12) and (13) used in this work are useful complements to the forms of α-preformation factors in Refs. [13,15,29,30,41].

III. NUMERICAL RESULTS AND DISCUSSIONS

A. Numerical results of α-decay half-lives for the observed $N = 125$, 126, and 127 isotones

In this section, we give theoretical results on the α-decay half-lives of the $N = 125$, 126, and 127 isotonic chains from Bi to Np by using the improved BMP cluster model introduced in Sec. II. The numerical results can be found in Table I. The first column represents the α-decay channels. The second and the third columns are the spins and parities of parent

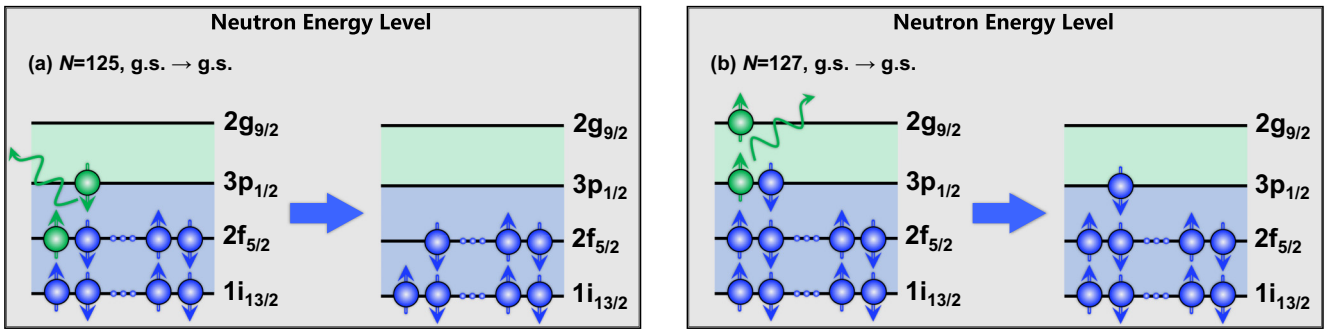

FIG. 1. The schematic description of the neutron-occupation change in the ground-state α decay of (a) the $N = 125$ isotones and (b) the $N = 127$ isotones. The black solid lines stand for the energy levels. The regions in blue denote the $N = 126$ magic core, while the regions in green denote the shell gap above $N = 126$. A circle with arrow on the line denotes the neutron with spin-up or spin-down state, in which the green circle denotes the neutron taken to form the α particle.

and daughter nuclei in ground state, while the fourth column denotes the orbital angular momentum carried by the α particles. The α-decay energies and the α-preformation factors are given in the fifth and sixth columns, respectively. The last three columns list the α-decay half-lives in the units of seconds, with $T_{1/2}^{\mathrm{Expt}}$ being the experimental half-lives, and $T_{1/2}^{\mathrm{C\text{-}P}}$ and $T_{1/2}^{\mathrm{Z\text{-}P}}$ being the theoretical half-lives calculated by the original BMP cluster model with the constant α-preformation factors and the improved BMP cluster model with the charge-dependent α-preformation factors, respectively. The α-decay energies are taken from Refs. [43,44], while the experimentally recommended values for α decay half-lives, spin, and parity are taken from Ref. [45]. For nuclei with multiple decay channels, the experimental half-lives $T_{1/2}^{\mathrm{Expt}}$ in Table I are obtained by

$$T_{1/2}^{\mathrm{Expt}} = T_{1/2}/\gamma_\alpha, \tag{14}$$

with $T_{1/2}$ being the measured half-life of the unstable nucleus given by Ref. [45] and γ_α being the branching ratio for α decay.

As mentioned before, the improved BMP cluster model makes use of the charge-dependent α-preformation factors in Eq. (13), whose explicit expressions for different categories of nuclei could be found in Table I. Take the $N = 126$ even-even isotonic chain as an example. P_α for the even-even isotones is found to be $P_\alpha = 0.0306(Z - 82)$. The nucleus with the minimal P_α in this isotonic chain is ^{210}Po, which has a small α-preformation factor of $P_\alpha = 0.0612$ due to the strong shell effect. Above ^{210}Po, P_α increases gradually with the valence proton number outside the $Z = 82$ shell up to the nucleus ^{218}U. The α-preformation factor of ^{218}U is the maximal one in this chain, which is found to be $P_\alpha = 0.306$.

From Table I, it can be seen that the α-preformation factors of even-even nuclei are noticeably larger than those of odd-A nuclei in $N = 126$ isotones. This could be explained qualitatively by the existence of the unpaired proton in odd-A nuclei with $N = 126$, which significantly weakens the pairing correlation and hinders the α clustering. Similar arguments could also be used to explain the observation that the odd-odd nuclei with the unpaired protons and neutrons have smaller α-preformation factors than the odd-A nuclei in $N = 125$ and 127 isotonic chains. Moreover, Table I shows that, the P_α values of $N = 127$ isotones are significantly smaller than those of $N = 125$ isotones. This can be explained by the fact that the valence neutrons in the $N = 125$ isotones are in the same major shell, while the valence neutrons of $N = 127$ isotones are in different major shells. It is thus more difficult

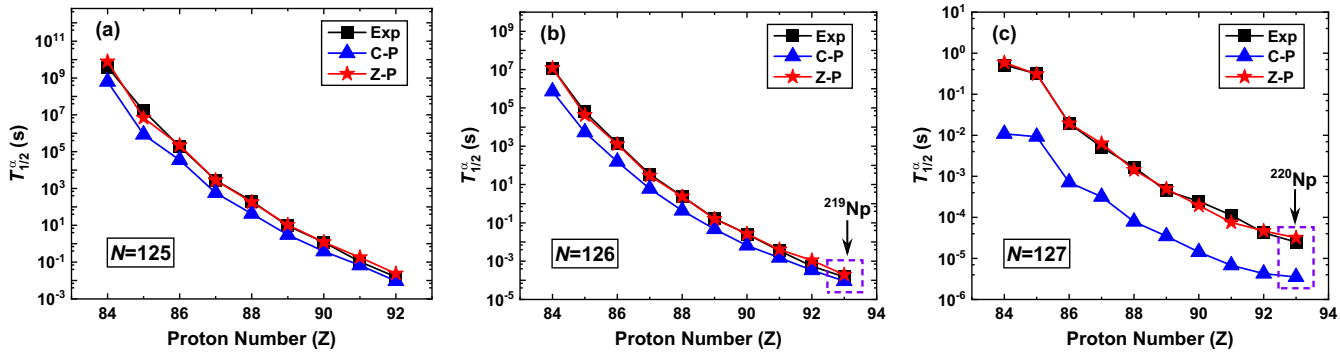

FIG. 2. The α-decay half-lives for (a) $N = 125$, (b) $N = 126$, and (c) $N = 127$ isotones versus the proton numbers. The black solid squares represent the experimental half-lives, the blue triangles represent the theoretical half-lives calculated by using the original BMP cluster model with constant α-preformation factors, and the red stars represent the theoretical half-lives calculated by using the improved BMP cluster model with charge-dependent α-preformation factors.

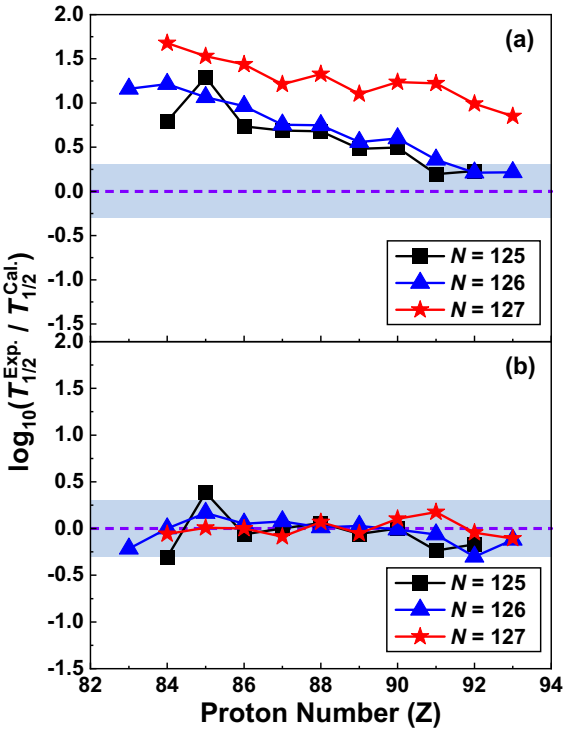

FIG. 3. The logarithmic hindrance factor given by (a) the original BMP cluster model with the constant α-preformation factors and (b) the improved BMP cluster model with the charge-dependent α-preformation factors versus the proton number for the α decay along $N = 125$, 126, and 127 isotonic chains. The blue band means that the hindrance factors are smaller than two in this region.

to form the α cluster for $N = 127$ isotones than the $N = 125$ isotones due to the neutron shell effect. This argument is also pictured in Fig. 1, with the arrangement of neutron energy levels taken from Ref. [46].

The experimental half-lives shown in Table I vary in a wide range from 2.50×10^{-5} to 6.00×10^{26} s. It can be seen straightforwardly that these experimental half-lives are well reproduced by the improved BMP cluster model with the charge-dependent α-preformation factors within a factor of $\approx$2. Noticeably, the theoretical results for the new isotopes ^{219,220}Np are in good agreement with the experimental data. The agreement between the theoretical half-lives and the experimental data along the $N = 125$, 126, and 127 isotonic chains can also been seen intuitively in Fig. 2. We also plot in the same figure the theoretical results given by the original BMP cluster model with the constant α-preformation factors.

In Fig. 3, the logarithmic hindrance factors $\delta = \log_{10}(T_{1/2}^{\mathrm{Expt}}/T_{1/2}^{\mathrm{Calc}})$ are plotted for the $N = 125$, 126, and 127 isotonic chains. The regions in blue correspond to the deviation between the theoretical half-lives and the experimental data within a factor of two. The δ values are far above the blue band in Fig. 3(a) given by the original BMP cluster model with the constant α-preformation factors, while almost all the δ values given by the improved BMP cluster model with the charge-dependent α-preformation factors in Fig. 3(b) lie within the blue band.

TABLE II. The rms deviations between the calculations and the latest experimental data from different works.

	Ref. [35]	Ref. [34]	Ref. [36]	This work
$\sqrt{\sigma^2}$	0.4456	0.4008	0.3822	0.1419

To systematically evaluate the agreements between the theoretical half-lives and the experimental data, we calculate the root-mean-square (rms) deviation

$$\sqrt{\sigma^2} = \sqrt{\sum_{i=1}^{n} \left[\log_{10}\left(T_{1/2}^{\mathrm{Expt},\,i}/T_{1/2}^{\mathrm{Calc},\,i}\right)\right]^2/n}. \quad (15)$$

The rms deviation for the original BMP cluster model with the constant α-preformation factors are 0.9602, while the rms deviation is reduced to 0.1419 for the improved BMP cluster model with the charge-dependent α-preformation factors. The results show that, with the charge-dependent α-preformation factors, the improved BMP cluster model gives theoretical results in much better agreement with experimental half-lives.

The α decays of $N = 125$, 126, and 127 isotones have also been studied in some previous works [34–36], where similar expressions for the charge-dependent α-preformation factors are used. For comparison, we calculate the rms deviations between their theoretical results and the latest experimental data for these works as well. Compared with the old experimental data used in Refs. [34–36], there are several important updates in the latest experimental data. The results are listed in Table II. It is straightforward to see that our work gives better results.

B. Quantitative predictions on the α-decay half-lives of $N = 125$, 126, 127 isotones with $94 \leqslant Z \leqslant 102$

In this subsection, we use the improved BMP cluster model with the charge-dependent α-preformation factors to make quantitative predictions on the α-decay half-lives of the undiscovered nuclei with $94 \leqslant Z \leqslant 102$ in the vicinity of the magic number $N = 126$. These results could be useful references for future experimental studies on the robustness of the magic number $N = 126$.

Here, three versions of the Weizsäcker-Skyrme (WS) mass formulas are adopted to calculate the theoretical α-decay energy, including the WS3 formula [47], the WS4 formula [48], and the WS4 formula with the radial-basis-function (RBF) corrections (abbreviated as the WS4$^{\mathrm{RBF}}$ formula) [48]. With the optimal parameters, the rms deviations between all the measured mass data and theoretical results of the WS3 formula, the WS4 formula, and the WS4$^{\mathrm{RBF}}$ formula are given by 336, 298, and 170 keV, respectively. The theoretical α-decay energy $Q_\alpha^{\mathrm{Theor}}$ is extracted from Ref. [49] by taking the relation

$$Q_\alpha^{\mathrm{Theor}} = \Delta M_p - (\Delta M_d + \Delta M_\alpha), \quad (16)$$

with ΔM_p, ΔM_d, and ΔM_α being the mass excesses of parent nucleus, daughter nucleus, and α particle, respectively. To see the local accuracy of the three mass formulas in the vicinity

TABLE III. Predictions of α-decay half-lives of the $N = 125$, 126, and 127 isotones with $94 \leqslant Z \leqslant 102$. $Q_\alpha^{\rm WS3}$, $Q_\alpha^{\rm WS4}$, and $Q_\alpha^{\rm WS4+RBF}$ represent the theoretical α-decay energy calculated by the WS3 formula, the WS4 formula, and the WS4 formula with the radial-basis-function (RBF) corrections, respectively. $T_{1/2}^{\rm WS3}$, $T_{1/2}^{\rm WS4}$, and $T_{1/2}^{\rm WS4+RBF}$ are the corresponding α decay half-life. The orbital angular momentum l_α in the second column are obtained from the trends of each isotonic chain shown in Table I. The nuclear mass tables with these WS formulas are taken from Ref. [49].

α decay	l_α	$Q_\alpha^{\rm WS3}$ (MeV)	$Q_\alpha^{\rm WS4}$ (MeV)	$Q_\alpha^{\rm WS4+RBF}$ (MeV)	P_α^Z	$T_{1/2}^{\rm WS3}$ (s)	$T_{1/2}^{\rm WS4}$ (s)	$T_{1/2}^{\rm WS4+RBF}$ (s)
			$N = 125$ (odd-A), $P_\alpha^Z = 0.0239(Z-82)$					
^{225}Fm $\rightarrow$ ^{221}Cf $+\alpha$	2	10.980	11.025	11.006	0.4302	3.39×10^{-6}	2.73×10^{-6}	2.99×10^{-6}
^{223}Cf $\rightarrow$ ^{219}Cm $+\alpha$	2	10.441	10.502	10.483	0.3824	1.31×10^{-5}	9.56×10^{-6}	1.05×10^{-6}
^{221}Cm $\rightarrow$ ^{217}Pu $+\alpha$	2	9.943	10.057	10.034	0.3346	4.58×10^{-5}	2.49×10^{-5}	2.82×10^{-5}
^{219}Pu $\rightarrow$ ^{215}U $+\alpha$	2	9.316	9.449	9.447	0.2868	3.88×10^{-4}	1.78×10^{-4}	1.82×10^{-4}
			$N = 125$ (odd-odd), $P_\alpha^Z = 0.0144(Z-82)$					
^{226}Md $\rightarrow$ ^{222}Es $+\alpha$	2	11.228	11.270	11.252	0.2736	3.31×10^{-6}	2.72×10^{-6}	2.97×10^{-6}
^{224}Es $\rightarrow$ ^{220}Bk $+\alpha$	2	10.689	10.712	10.693	0.2448	1.21×10^{-5}	1.08×10^{-5}	1.18×10^{-5}
^{222}Bk $\rightarrow$ ^{218}Am $+\alpha$	2	10.204	10.297	10.276	0.2160	3.76×10^{-5}	2.31×10^{-5}	2.58×10^{-5}
^{220}Am $\rightarrow$ ^{216}Np $+\alpha$	2	9.661	9.768	9.754	0.1872	1.80×10^{-4}	9.93×10^{-5}	1.07×10^{-4}
^{218}Np $\rightarrow$ ^{214}Pa $+\alpha$	2	8.899	9.063	9.138	0.1584	3.90×10^{-3}	1.43×10^{-3}	9.05×10^{-4}
			$N = 126$ (even-even), $P_\alpha^Z = 0.0306(Z-82)$					
^{228}No $\rightarrow$ ^{224}Fm $+\alpha$	0	11.629	11.627	11.604	0.6120	2.84×10^{-7}	2.86×10^{-7}	3.18×10^{-7}
^{226}Fm $\rightarrow$ ^{222}Cf $+\alpha$	0	11.114	11.077	11.055	0.5508	8.36×10^{-7}	9.96×10^{-7}	1.11×10^{-7}
^{224}Cf $\rightarrow$ ^{220}Cm $+\alpha$	0	10.632	10.663	10.644	0.4896	2.30×10^{-6}	1.97×10^{-6}	2.17×10^{-6}
^{222}Cm $\rightarrow$ ^{218}Pu $+\alpha$	0	9.983	10.079	10.071	0.4284	1.69×10^{-5}	1.02×10^{-6}	1.06×10^{-5}
^{220}Pu $\rightarrow$ ^{216}U $+\alpha$	0	9.285	9.398	9.490	0.3672	2.10×10^{-4}	1.09×10^{-5}	6.40×10^{-5}
			$N = 126$ (odd-A), $P_\alpha^Z = 0.0252(Z-82)$					
^{227}Md $\rightarrow$ ^{223}Es $+\alpha$	0	11.314	11.331	11.308	0.4788	7.62×10^{-7}	7.05×10^{-7}	7.84×10^{-7}
^{225}Es $\rightarrow$ ^{221}Bk $+\alpha$	0	10.905	10.870	10.849	0.4284	1.43×10^{-6}	1.69×10^{-6}	1.88×10^{-6}
^{223}Bk $\rightarrow$ ^{219}Am $+\alpha$	0	10.308	10.383	10.367	0.3780	7.38×10^{-6}	5.03×10^{-6}	5.44×10^{-6}
^{221}Am $\rightarrow$ ^{217}Np $+\alpha$	0	9.652	9.757	9.758	0.3276	6.29×10^{-5}	3.50×10^{-5}	3.50×10^{-5}
			$N = 127$ (odd-A), $P_\alpha^Z = 0.0055(Z-82)$					
^{229}No $\rightarrow$ ^{225}Fm $+\alpha$	5	12.137	12.122	12.095	0.1100	6.73×10^{-7}	7.14×10^{-7}	8.02×10^{-7}
^{227}Fm $\rightarrow$ ^{223}Cf $+\alpha$	5	11.604	11.481	11.455	0.0990	2.05×10^{-6}	3.51×10^{-6}	3.95×10^{-6}
^{225}Cf $\rightarrow$ ^{221}Cm $+\alpha$	5	11.209	11.049	11.031	0.0880	3.70×10^{-6}	7.63×10^{-6}	8.28×10^{-6}
^{223}Cm $\rightarrow$ ^{219}Pu $+\alpha$	5	10.580	10.555	10.538	0.0770	2.18×10^{-5}	2.45×10^{-5}	2.64×10^{-5}
^{221}Pu $\rightarrow$ ^{217}U $+\alpha$	5	10.214	10.093	10.015	0.0660	3.99×10^{-5}	7.36×10^{-5}	6.93×10^{-5}
			$N = 127$ (odd-odd), $P_\alpha^Z = 0.0035(Z-82)$					
^{228}Md $\rightarrow$ ^{224}Es $+\alpha$	5	11.819	11.786	11.759	0.0665	2.27×10^{-6}	2.61×10^{-6}	2.94×10^{-6}
^{226}Es $\rightarrow$ ^{222}Bk $+\alpha$	5	11.416	11.263	11.240	0.0595	4.10×10^{-6}	8.15×10^{-6}	9.03×10^{-6}
^{224}Bk $\rightarrow$ ^{220}Am $+\alpha$	5	10.847	10.792	10.782	0.0525	1.70×10^{-5}	2.19×10^{-5}	2.31×10^{-5}
^{222}Am $\rightarrow$ ^{218}Np $+\alpha$	5	10.400	10.308	10.340	0.0455	4.56×10^{-5}	7.20×10^{-5}	6.14×10^{-5}

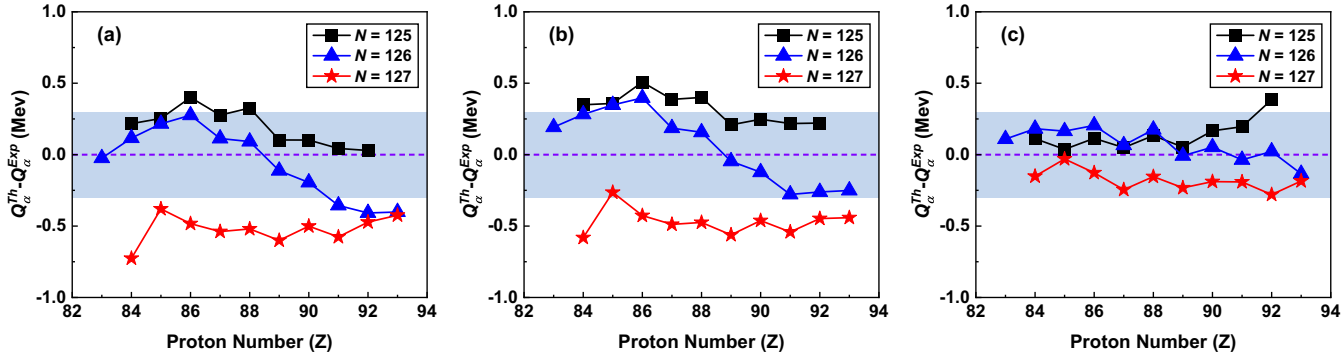

FIG. 4. The deviation between the calculated mass and the experimental data given by (a) the WS3 formula, (b) the WS4 formula, and (c) the WS4$^{\rm RBF}$ formula of the $N = 125$, 126, and 127 isotones. The blue band denotes the deviation between the theoretical α-decay energy and the experimental data in this region is smaller than 300 keV.

of the major number $N = 126$, we plot the deviation between the theoretical α-decay energy $Q_\alpha^{\rm Theor}$ and the experimental data $Q_\alpha^{\rm Expt}$ of the $N = 125$, 126, and 127 isotones for the WS3 formula, the WS4 formula, and the WS4$^{\rm RBF}$ formula in Fig. 4. It is shown that, compared with the other two formulas, the results given by the WS4$^{\rm RBF}$ formula agree better with the experimental data. Then, we predict the α-decay half-lives of some $N = 125$, 126, and 127 isotones with $94 \leqslant Z \leqslant 102$ by using the improved BMP cluster model, with the results listed in Table III. We expect that these predictions could be helpful for future experimental studies.

IV. SUMMARY

In conclusion, we have studied the α decay of the $N = 125$, 126, and 127 isotones, including the new isotopes ^{219,220}Np, by using the improved BMP cluster model with charge-dependent α-preformation factors. Compared with the original BMP cluster model with the constant α-preformation factors, the improved BMP cluster model gives better descriptions of the α-decay half-lives in the vicinity of the neutron magic number $N = 126$. In general, the theoretical results agree with the experimental values within a factor of two. Noticeably, the theoretical half-lives are in good agreement with the experimental data for the new isotopes ^{219,220}Np. Furthermore, with the updated parameter in the charge-dependent α-preformation factors, the calculation of the improved BMP cluster model also shows better agreement with the latest experimental data than previous work. All of these show that the improved BMP cluster model is indeed a reliable theoretical model for α decays in this mass region.

For the convenience of future experimental studies on the robustness of the magic number $N = 126$, we also provide theoretical predictions of the α-decay half-lives for the $N = 125$, 126, and 127 isotones with $94 \leqslant Z \leqslant 102$. It is expected that these results could be useful references.

ACKNOWLEDGMENTS

This work was supported by the National Natural Science Foundation of China (Grants No. 11975167, No. 11535004, No. 11947211, No. 11905103, No. 11761161001, No. 11375086, No. 11565010, No. 11881240623, and No. 11961141003), by the National Key R&D Program of China (Contracts No. 2018YFA0404403 and No. 2016YFE0129300), by the Science and Technology Development Fund of Macau under Grant No. 008/2017/AFJ, by the Fundamental Research Funds for the Central Universities (Grant No. 22120200101), and by China Postdoctoral Science Foundation (Grant No. 2019M660095).

[1] R. G. Lovas, R. J. Liotta, A. Insolia, K. Varga, and D. S. Delion, Phys. Rep. **294**, 265 (1998).
[2] D. S. Delion, Zhongzhou Ren, A. Dumitrescu, and D. Ni, J. Phys. G **45**, 053001 (2018).
[3] C. Qi, R. Liotta, and R. Wyss, Prog. Part. Nucl. Phys. **105**, 214 (2019).
[4] Z. Ren and B. Zhou, Front. Phys. **13**, 132110 (2018).
[5] B. Buck, A. C. Merchant, and S. M. Perez, Phys. Rev. Lett. **65**, 2975 (1990).
[6] B. Buck, A. C. Merchant, and S. M. Perez, Phys. Rev. C **45**, 2247 (1992).
[7] B. Buck, A. C. Merchant, and S. M. Perez, At. Data Nucl. Data Tables **54**, 53 (1993).
[8] K. Varga, R. G. Lovas, and R. J. Liotta, Phys. Rev. Lett. **69**, 37 (1992).
[9] K. Varga, R. G. Lovas, and R. J. Liotta, Nucl. Phys. A **550**, 421 (1992).
[10] C. Xu and Z. Ren, Nucl. Phys. A **753**, 174 (2005).
[11] P. Mohr, Phys. Rev. C **73**, 031301(R) (2006).
[12] D. Ni and Z. Ren, Nucl. Phys. A **828**, 348 (2009).
[13] G. Röpke, P. Schuck, Y. Funaki, H. Horiuchi, Z. Ren, A. Tohsaki, C. Xu, T. Yamada, and B. Zhou, Phys. Rev. C **90**, 034304 (2014).
[14] V. Y. Denisov, O. I. Davidovskaya, and I. Y. Sedykh, Phys. Rev. C **92**, 014602 (2015).
[15] D. Bai, Z. Ren, and G. Röpke, Phys. Rev. C **99**, 034305 (2019).
[16] V. V. Baran and D. S. Delion, Phys. Rev. C **99**, 031303(R) (2019).
[17] C. Xu, G. Ropke, P. Schuck, Z. Ren, Y. Funaki, H. Horiuchi, A. Tohsaki, T. Yamada, and B. Zhou, Phys. Rev. C **95**, 061306(R) (2017).
[18] B. A. Brown, Phys. Rev. C **46**, 811 (1992).
[19] Y. Hatsukawa, H. Nakahara, and D. C. Hoffman, Phys. Rev. C **42**, 674 (1990).
[20] M. Ismail, W. M. Seif, W. M. Tawfik, and A. M. Hussein, Ann. Phys. (NY) **406**, 1 (2019).
[21] A. N. Andreyev *et al.*, Phys. Rev. Lett. **110**, 242502 (2013).
[22] J. Khuyagbaatar *et al.*, Phys. Rev. Lett. **115**, 242502 (2015).
[23] H. B. Yang *et al.*, Phys. Lett. B **777**, 212 (2018).
[24] Z. Y. Zhang *et al.*, Phys. Rev. Lett. **122**, 192503 (2019).
[25] D. Bai and Z. Ren, Phys. Lett. B **786**, 5 (2018).
[26] D. Bai and Z. Ren, Eur. Phys. J. A **54**, 220 (2018).
[27] M. A. Souza, H. Miyake, T. Borello-Lewin, C. A. da Rocha, and C. Frajuca, Phys. Lett. B **793**, 8 (2019).
[28] K. Auranen *et al.*, Phys. Rev. Lett. **121**, 182501 (2018).
[29] C. Xu, Z. Ren, G. Röpke, P. Schuck, Y. Funaki, H. Horiuchi, A. Tohsaki, T. Yamada, and B. Zhou, Phys. Rev. C **93**, 011306(R) (2016).
[30] H. F. Zhang, G. Royer, Y. J. Wang, J. M. Dong, W. Zuo, and J. Q. Li, Phys. Rev. C **80**, 057301 (2009).
[31] Z. Ren and G. Xu, Phys. Rev. C **36**, 456 (1987).
[32] Z. Ren and G. Xu, Phys. Rev. C **38**, 1078 (1988).
[33] Z. Ren and G. Xu, J. Phys. G **15**, 465 (1989).
[34] D. Ni and Z. Ren, Phys. Rev. C **80**, 014314 (2009).
[35] C. Xu and Z. Ren, Phys. Rev. C **76**, 027303 (2007).
[36] Y. Qian and Z. Ren, Nucl. Phys. A **852**, 82 (2011).
[37] C. Xu and Z. Ren, Phys. Rev. C **68**, 034319 (2003).
[38] K. Wildermuth and Y. C. Tang, *A Unified Theory of the Nucleus* (Academic Press, New York, 1977).
[39] R. E. Langer, Phys. Rev. **51**, 669 (1937).
[40] S. A. Gurvitz and G. Kalbermann, Phys. Rev. Lett. **59**, 262 (1987).

[41] D. Deng and Z. Ren, Phys. Rev. C **93**, 044326 (2016).
[42] National Nuclear Data Center: https://www.nndc.bnl.gov.
[43] W. J. Huang, G. Audi, M. Wang, F. G. Kondev, S. Naimi, and X. Xu, Chin. Phys. C **41**, 030002 (2017).
[44] M. Wang, G. Audi, F. G. Kondev, W. J. Huang, S. Naimi, and X. Xu, Chin. Phys. C **41**, 030003 (2017).
[45] G. Audi, F. G. Kondev, Meng Wang, W. J. Huang, and S. Naimi, Chin. Phys. C **41**, 030001 (2017).
[46] N. Schwierz, I. Wiedenhover, and A. Volya, arXiv:0709.3525.
[47] M. Liu *et al.*, Phys. Rev. C **84**, 014333 (2011).
[48] N. Wang *et al.*, Phys. Lett. B **734**, 215 (2014).
[49] Weizsäcker-Skyrme Nuclear Mass Tables: http://www.imqmd.com/mass/.